FRIB Summer School Lecture on "Kilonovae"

Brian D. Metzger
Columbia Astrophysics Laboratory
Columbia University
bmetzger@phys.columbia.edu

May 14, 2018

Abstract

Lecture to be delivered at the FRIB summer school on binary neutron star mergers, held on May 16-18, 2018 at Michigan State University.

Kilonovae in a Nutshell

• BNS mergers eject neutron-rich matter, through a variety of different channels (tidal tails, magnetar winds, accretion disk outflows, etc.) on timescales of milliseconds to seconds, which thereafter freely expands into space (Fig. 1).

• As ejecta decompresses, heavy elements (atomic mass number $A \gtrsim 120$) are synthesized by the rapid capture of neutrons onto seed nuclei.

• Synthesized isotopes are radioactive, and decay through β-decays ($A \rightarrow A^* + e^- + \bar{\nu}_e$), α-decays ($A \rightarrow A^* + \alpha$), and fission ($A \rightarrow A' + A''$), over a range of timescales.

• The decay products transfer their energy to the ejecta (through e.g. coulomb collisions), keeping it warmer than otherwise had it instead cooled adiabatically.

• Thermal radiation escapes from the (radioactively-heated) expanding ejecta, powering the kilonova emission we observe. The peak luminosity is proportional to the quantity of radioactive isotopes synthesized.

• The wavelength and evolution timescale of the light curves depend on the composition of the ejecta. Broadly, the emission color is "red" or "blue" depending on whether the ejecta contains lanthanide/actinide nuclei or exclusively lighter nuclei.

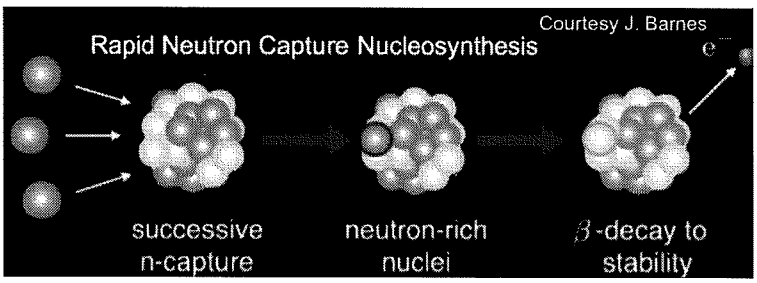

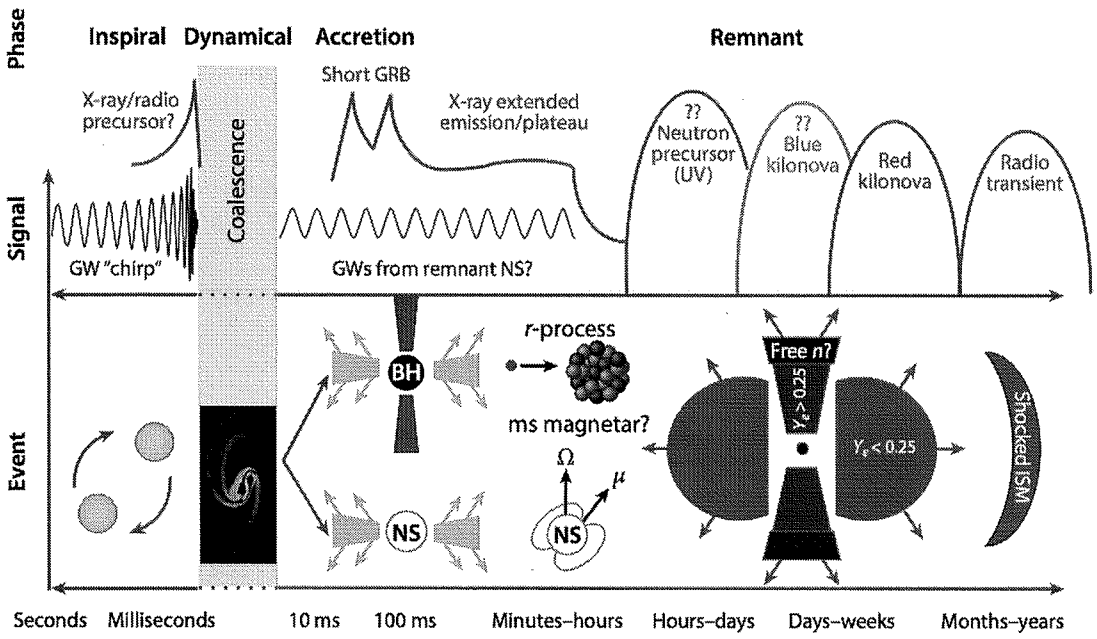

Figure 1: Timeline of BNS mergers and their electromagnetic counterparts (Fernández & Metzger 2016).

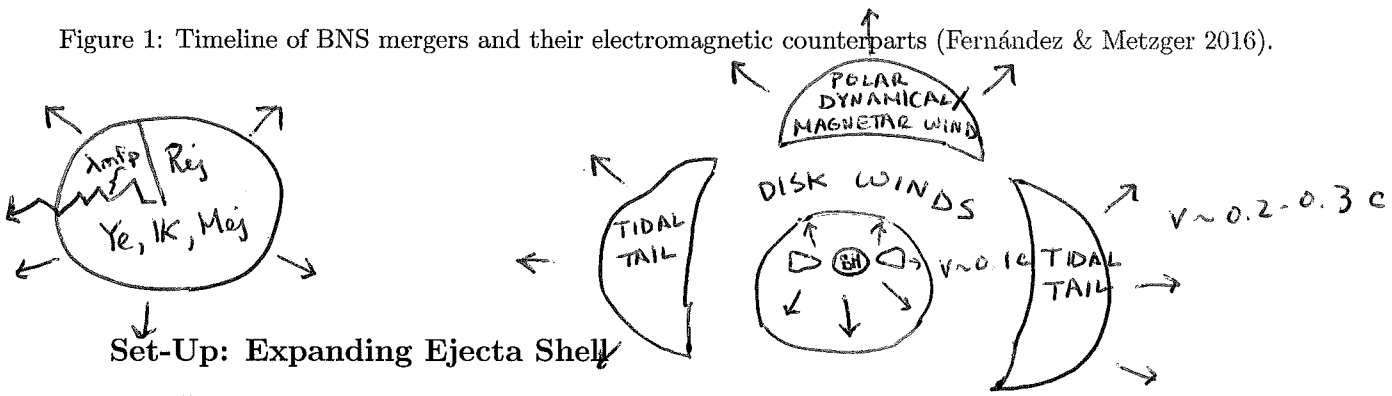

Set-Up: Expanding Ejecta Shell

• Different ejecta components have distinct masses, velocities, geometries, and compositions (light or heavy r-process nuclei, depending on Y_e), see Table 1.

• We first develop a spherically-symmetric model for a single ejecta component. At the end we return to how different ejecta components interact with one another.

Consider an expanding shell of mass $M_{\rm ej}$ and mean velocity $v_{\rm ej}$.
The characteristic radius of the ejecta at time t after the merger is

$$R_{\rm ej} = v_{\rm ej} t \approx 3 \times 10^{14}\,{\rm cm} \left(\frac{v_{\rm ej}}{0.1\,c}\right) \left(\frac{t}{1\,{\rm day}}\right) \quad (1)$$

The mean density of the shell is

$$\rho_{\rm ej} = \frac{M_{\rm ej}}{(4\pi/3) R_{\rm ej}^3} \approx 3 \times 10^{-13}\,{\rm g\,cm^{-3}} \left(\frac{M_{\rm ej}}{0.01 M_\odot}\right) \left(\frac{v_{\rm ej}}{0.1\,c}\right)^{-3} \left(\frac{t}{1\,{\rm day}}\right)^{-3}$$

The radial optical depth (# of photon mean free-paths $\lambda_{\rm mfp}$) through the ejecta is

$$\tau_{\rm ej} = \frac{R_{\rm ej}}{\lambda_{\rm mfp}} \approx \rho_{\rm ej} \kappa R_{\rm ej} \approx 73 \left(\frac{\kappa}{1\,{\rm cm^2\,g^{-1}}}\right) \left(\frac{M_{\rm ej}}{0.01 M_\odot}\right) \left(\frac{v_{\rm ej}}{0.1\,c}\right)^{-2} \left(\frac{t}{1\,{\rm day}}\right)^{-2}, \quad (2)$$

where κ is the opacity (cross section per unit mass of absorbing material).

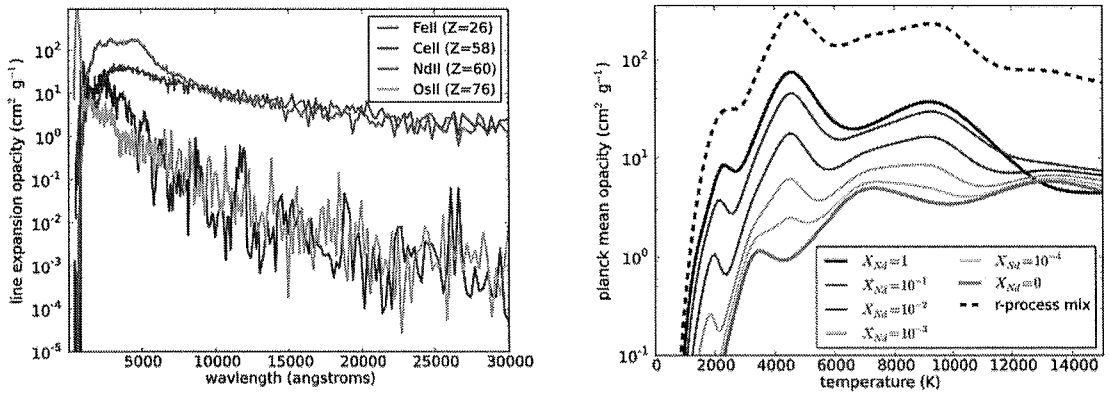

Figure 2: **Left:** Line opacity as a function of wavelength, comparing elements with d-shell valence shell electrons (iron, cerium) to lanthanides with f-shell electrons (e.g. Nd, Os). **Right:** Planck mean opacities, $\kappa_{\rm Pl} = \frac{\int_0^\infty \kappa_\nu B_\nu(T) d\nu}{\int_0^\infty B_\nu(T) d\nu}$, for ejecta containing different mass fractions of lanthanides $X_{\rm Nd}$, the remainder being non-lanthanides $X_{\rm Fe} = 1 - X_{\rm Nd}$. From Kasen et al. (2013).

Opacities

• Main source of opacity at optical and infrared wavelengths is a "forrest" of bound-bound atomic (line) transitions densely spaced in wavelength.

• The number of lines, and thus the opacity, depends on the atomic complexity of the ejecta. Roughly, the number of atomic levels is given by the possible combinations of ways to place n valence electrons into g states (level degeneracy), i.e.

$$N_{\rm lev} \sim \frac{g!}{n!(g-n)!}; \quad N_{\rm lines} \sim N_{\rm lev}^2 \qquad (3)$$

Fe$^+$ ← 5 valence electrons

g = 10

$N_{\rm lev} \sim \frac{10!}{(5!)(5!)} = 252$

lanthanide

g = 14

$N_{\rm lev} \sim \frac{14!}{(7!)(7!)} = 3432$

There are many more ways to distribute the valence electrons in atoms with partially-filled open f shell (lanthanides/actinides; degeneracy $g = 14$) than for atoms with d shell (iron or light r-process elements; $g = 10$).

• The line opacity of matter containing even a modest mass fraction of lanthanides (atomic number $A \sim 138 - 174$; $Y_e \lesssim 0.25$) is orders of magnitude higher than one containing exclusively light r-process nuclei ($A \lesssim 138$; $Y_e \gtrsim 0.25$). See Fig. 2.

• Coincidentally, an important nuclear physics threshold (r-process nucleosyntehsis past the second mass peak at $A \sim 130$) also corresponds to an important *atomic physics* transition (from simple to complex atomic structure).

• For analytic estimates, we take *grey* opacities

$$\kappa_{\rm Fe} \sim 0.1\, cm^2\, g^{-1}; \; \kappa_{\rm light-r} \sim 1\, cm^2\, g^{-1}; \; \kappa_{\rm heavy-r} \sim 10\, cm^2\, g^{-1},$$

This is OK for calculating **bolometric** light curves, i.e. integrated over all frequencies. However, full multi-frequency radiative transfer simulations are needed to accurately calculate light curves in given observing bands.

Basics of Photon Diffusion

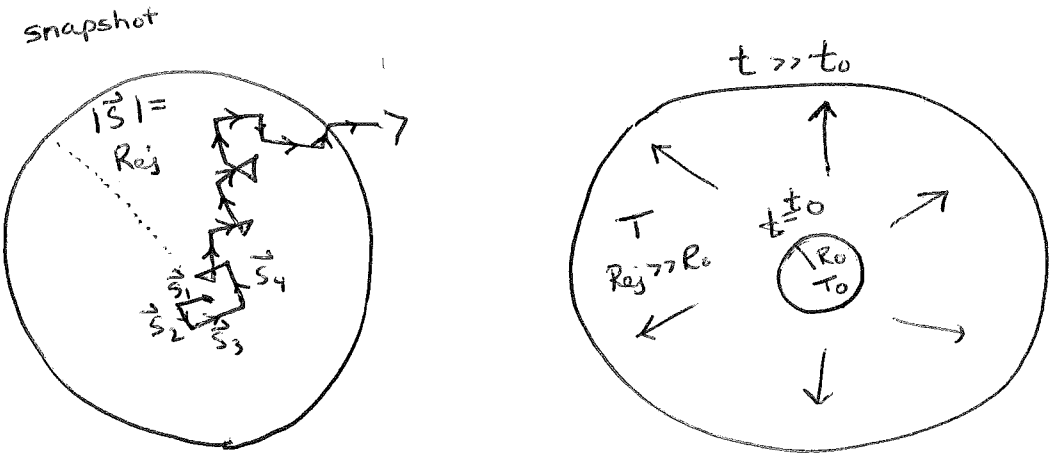

The mean-free-path and optical depth of the ejecta at a given time are

$$\lambda_{\rm mfp} = \frac{1}{\rho_{\rm ej}\kappa}; \quad \tau_{\rm ej} = \frac{R_{\rm ej}}{\lambda_{\rm mfp}}$$

After $N \gg 1$ scatterings, a photon undergoes a total displacement

$$\vec{S} = \sum_i^N \vec{s}_i,$$

where on average $|\vec{s}_i| = \lambda_{\rm mfp}$. Thus we have a random walk,

$$|S|^2 = \vec{S}\cdot\vec{S} = \sum_{i=j}^N \vec{s}_i\cdot\vec{s}_j + \sum_{j\neq i}^N \vec{s}_i\cdot\vec{s}_j \underset{\text{average}}{=} \sum_{i=j}^N \vec{s}_i\cdot\vec{s}_j = N s_i^2 = N\lambda_{\rm mfp}^2$$

In other words, $N = |S|^2/\lambda_{\rm mfp}^2$ scatterings are required to diffuse a distance $|S|$.

Since the time between a single scattering is $\lambda_{\rm mfp}/c$, the "diffusion" time for photons to escape the ejecta of radial thickness $R_{\rm ej} = |S| = N^{1/2}\lambda_{\rm mfp}$ is given by

$$t_{\rm diff} = N\frac{\lambda_{\rm mfp}}{c} = \frac{R_{\rm ej}^2}{\lambda_{\rm mfp}^2}\frac{\lambda_{\rm mfp}}{c} = \frac{R_{\rm ej}}{\lambda_{\rm mfp}}\frac{R_{\rm ej}}{c} = \tau_{\rm ej}\frac{R_{\rm ej}}{c},$$

Using equations (1), (2), we find numerically that

$$t_{\rm diff} \approx \tau_{\rm ej}\frac{R_{\rm ej}}{c} \approx 7.3\ {\rm days}\left(\frac{\kappa}{1\,{\rm cm^2\,g^{-1}}}\right)\left(\frac{M_{\rm ej}}{0.01 M_\odot}\right)\left(\frac{v_{\rm ej}}{0.1\,c}\right)^{-1}\left(\frac{t}{1\,{\rm day}}\right)^{-1}, \quad (4)$$

This can also be approached more formally by considering the radiation energy flux in the diffusion approximation

$$\vec{F} = \frac{c}{\kappa\rho}\frac{d}{dr}\left(\frac{aT^4}{3}\right) \Rightarrow L_{\rm r} = 4\pi r^2|\vec{F}| \sim \frac{aT^4}{t_{\rm diff}}R^3 \quad (5)$$

Peak of the Light Curve

Note that $t_{\rm diff} \propto t^{-1}$, resulting in two distinct epochs in time:

$$t_{\rm diff} \gg t, \quad \text{Photons still trapped,} \quad t \ll t_{\rm peak},$$
$$t_{\rm diff} \ll t, \quad \text{Photons diffusive,} \quad t \gg t_{\rm peak},$$

where $t_{\rm peak}$ is the critical time at which $t_{\rm diff} = t$, i.e. when $\tau_{\rm ej} = c/v_{\rm ej}$,

$$t_{\rm peak} \approx \left(\frac{3\kappa M_{\rm ej}}{4\pi v_{\rm ej} c}\right)^{1/2} \approx 2.7 \text{ days} \left(\frac{\kappa}{1\,{\rm cm^2\,g^{-1}}}\right)^{1/2} \left(\frac{M_{\rm ej}}{0.01 M_\odot}\right)^{1/2} \left(\frac{v_{\rm ej}}{0.1\,c}\right)^{-1/2}. \quad (6)$$

We call this the "peak" time since it will correspond to the peak of the kilonova light curve.
The ejecta radius at peak light is

$$R_{\rm peak} = t_{\rm peak} v_{\rm ej} \approx 7 \times 10^{14} {\rm cm} \left(\frac{\kappa}{1\,{\rm cm^2\,g^{-1}}}\right)^{1/2} \left(\frac{M_{\rm ej}}{0.01 M_\odot}\right)^{1/2} \left(\frac{v_{\rm ej}}{0.1\,c}\right)^{1/2}, \quad (7)$$

i.e. 8 orders of magnitude larger than the size at ejection!

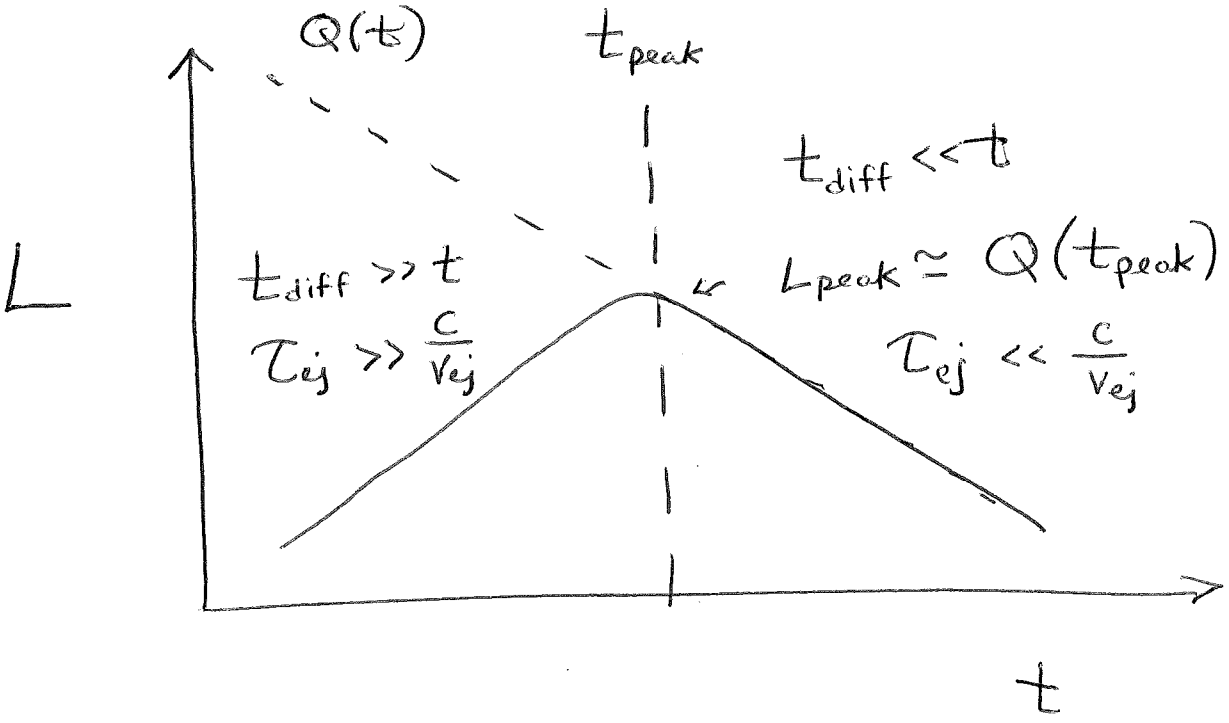

Pure Explosion (No Radioactivity)

First consider a case with zero radioactive heating.
We will show this is inadequate to explain the luminosity of GW170817.

• The energy density in radiation $u_{\rm rad} = aT^4$ in supernovae (and kilonovae) usually dominates that of matter, $u_{\rm matter} \propto \rho_{\rm ej} kT$, where T is the temperature.
While photons are still trapped ($t \ll t_{\rm peak}$), the internal energy is thus

$$E_{\rm th} \approx \frac{4\pi}{3} R_{\rm ej}^3 a T^4$$

• If the thermal energy of the ejecta is comparable to its kinetic energy, i.e. $E_0 \approx M_{\rm ej} v_{\rm ej}^2/2$, then the temperature at the time of ejection is

$$T_0 = \left(\frac{3E_0}{4\pi a R_0^3}\right)^{1/4} \approx \left(\frac{3M_{\rm ej} v_{\rm ej}^2}{8\pi a R_0^3}\right)^{1/4} \sim 4 \times 10^{10}\,{\rm K}$$

where we have taken $v_{\rm ej} = 0.1$ c, $M_{\rm ej} = 0.01 M_\odot$ and $R_0 = 100$ km.

• While photons are trapped ($t \ll t_{\rm peak}$), the ejecta expands adiabatically (for a $\gamma = 4/3$ gas, $E_{\rm th} \propto P_{\rm rad} \propto \rho^\gamma = \rho_{\rm ej}^{4/3} \propto R_{\rm ej}^{-4}$) and thus the internal energy drops

$$E_{\rm th} = E_0 \left(\frac{R_{\rm ej}}{R_0}\right)^{-1} \; ; \; T = T_0 \left(\frac{R_{\rm ej}}{R_0}\right)^{-1} \tag{8}$$

where E_0 and R_0 are the thermal energy and radius at the time of ejection, t_0.

• The thermal energy remaining **once radiation can escape** is much smaller

$$E_{\rm th}(t_{\rm peak}) \sim \frac{M_{\rm ej} v_{\rm ej}^2}{2} \frac{R_0}{R_{\rm peak}} \approx 10^{42}{\rm erg} \left(\frac{R_0}{100\,{\rm km}}\right) \left(\frac{\kappa}{1\,{\rm cm^2\,g^{-1}}}\right)^{-1/2} \left(\frac{M_{\rm ej}}{0.01 M_\odot}\right)^{1/2} \left(\frac{v_{\rm ej}}{0.1\,c}\right)^{3/2},$$

where we have used equation (8).
As this energy escapes over a time $\sim t_{\rm peak}$ (eq. 6), the peak luminosity **due exclusively to the initial thermal energy** is

$$L_{\rm peak}^{\rm zero\,r-process} \approx \frac{E_{\rm th}(t_{\rm peak})}{t_{\rm peak}} \approx 6 \times 10^{36} {\rm erg\,s^{-1}} \left(\frac{R_0}{100\,{\rm km}}\right) \left(\frac{\kappa}{1\,{\rm cm^2\,g^{-1}}}\right)^{-1} \left(\frac{v_{\rm ej}}{0.1\,c}\right)^2,$$

i.e. five orders of magnitude lower than the observed luminosities of GW170817, $L \approx 10^{41} - 10^{42}$ erg s^{-1} (Fig. 4).
• Clearly, something is keeping the ejecta hotter (hint: its radioactive).

• However, note that $L_{\rm peak} \propto R_0$. If something (e.g. a relativistic GRB jet) were to re-heat the ejecta at sufficiently late times $t_{\rm late} \gtrsim 1$ s (large $R_0 = v_{\rm ej} t_{\rm late}$), then the "initial" thermal energy might be relevant (referred by some as "cocoon" emission).

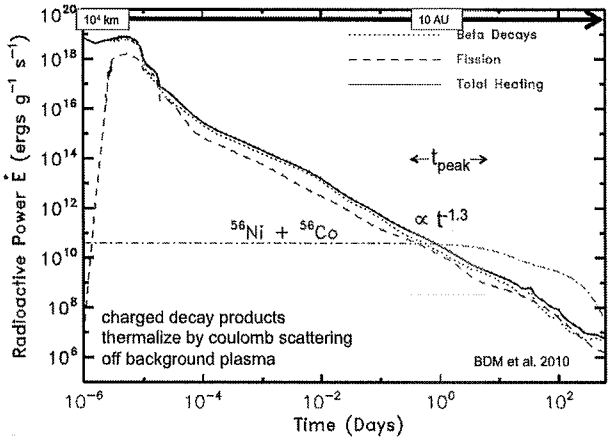

Figure 3: Radioactive heating rate $\dot{q}_r(t)$ from decay of r-process nuclei as a function of time t since ejection (or equivalently ejecta radius; shown at top). Also marked are the range of timescales $t \sim t_{\rm peak} \sim 0.5 - 5$ d (eq. 6) relevant to powering the kilonova emission. From Metzger et al. (2010).

Radioactivity

Radioactivity from decay r-process nuclei contributes an additional heating source, which per unit mass is (Fig. 3)

$$\dot{q}_r(t) \approx 10^{10} \epsilon_{\rm th} \left(\frac{t}{1\,{\rm day}} \right)^{-1.3} \ {\rm erg\,s^{-1}g^{-1}}, \quad Y_e \lesssim 0.35 \tag{9}$$

where $\epsilon_{\rm th} < 1$ is the thermalization efficiency.
The total heating rate (for the entire ejecta) is given by

$$\dot{Q}(t) = \dot{q}_r M_{\rm ej} \approx 2 \times 10^{41}\,{\rm erg\,s^{-1}} \left(\frac{M_{\rm ej}}{10^{-2} M_\odot} \right) \left(\frac{t}{1\,{\rm day}} \right)^{-1.3} \tag{10}$$

The peak luminosity of the kilonova is set by the radioactive heating at $t_{\rm peak}$ (eq. 6),

$$L_{\rm peak} \approx \dot{Q}(t_{\rm peak}) \approx 5 \times 10^{40}\,{\rm erg\,s^{-1}} \epsilon_{\rm th} \left(\frac{M_{\rm ej}}{0.01 M_\odot} \right)^{0.35} \left(\frac{v_{\rm ej}}{0.1\,c} \right)^{0.65} \left(\frac{\kappa}{1\,{\rm cm^2\,g^{-1}}} \right)^{-0.65} \tag{11}$$

The effective temperature of the emission at peak time is given by

$$T_{\rm peak} = \left(\frac{L_{\rm peak}}{4\pi\sigma R_{\rm peak}^2} \right)^{1/4} \approx 3460\,{\rm K}\ \epsilon_{\rm th}^{1/4} \left(\frac{M_{\rm ej}}{10^{-2} M_\odot} \right)^{-0.17} \left(\frac{v_{\rm ej}}{0.1\,c} \right)^{-0.09} \left(\frac{\kappa}{1\,{\rm cm^2\,g^{-1}}} \right)^{-0.41} \tag{12}$$

Equations (11) and (6) provide the peak luminosity, timescale, and effective temperature of the kilonova emission.

- All else being equal, a **larger** ejecta mass **increases** the peak luminosity and peak timescale of the emission.

- A **higher velocity increases** the peak luminosity and **decreases** the peak timescale.

- Ejecta containing heavy r-process nuclei (high opacity) produces emission with a longer timescale, lower luminosity, and lower temperature as compared to one with exclusively light r-process nuclei.

This is the basis for the distinction between "red" and "blue" kilonovae (Fig. 1).

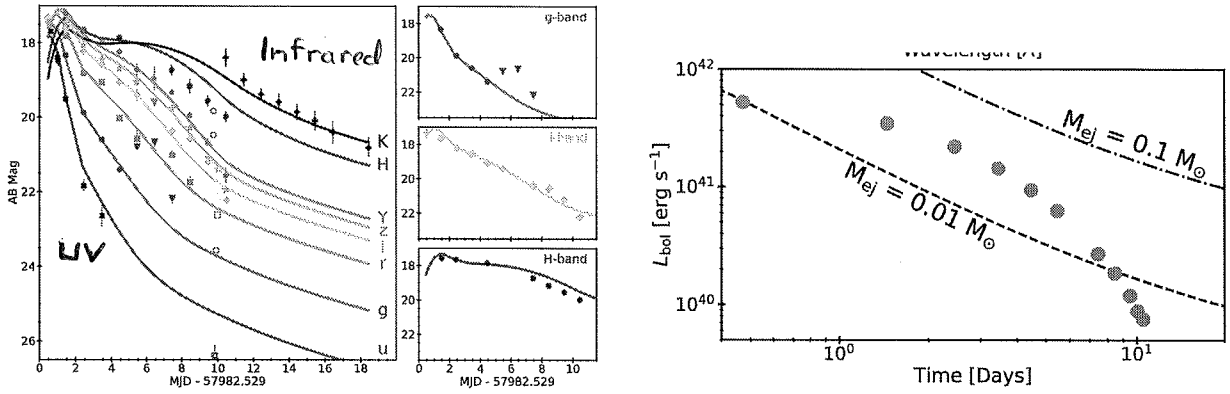

Figure 4: Kilonova light curves in different spectral bands (left panel) and bolometrically (right panel). Dot-dashed lines on the right show the total radioactive heating rate $\dot{Q}(t)$ (eq. 10) for $0.01M_\odot$ and $0.1M_\odot$ of r-process material as marked. From Cowperthwaite et al. (2017).

• Complex ejecta structure (e.g. multiple ejecta sources) can be crudely modeled by adding together separately the light curves from for each component.

• However, in a 1D model, ejecta components with larger velocity (larger radii) must have lower opacity than slower components (small radii).
Physically, high-opacity "red" ejecta blocks the visual light from "blue" ejecta.

GW170817

• Comparison between the observed bolometric light curve and the total r-process heating rate (eq. 10) provides a minimum on the ejecta mass of a few $\times 10^{-2} M_\odot$ (right panel of Fig. 4).

• Modeling the multi-band light curve of GW170817 requires at least two separate ejecta components with different composition (high and low opacities). One such fit is shown in the left panel of Fig. 4.

• Observed "blue" (visual wavelength; $T_{\rm eff} \approx 5000$ K) luminosity of $L_{\rm blue} \sim few \times 10^{41}$ erg s^{-1} and duration $t_{\rm peak} \sim 1$ day explained by $M_{\rm blue} \approx 0.02 M_\odot$, $v_{\rm blue} \approx 0.3$ c, $\kappa_{\rm light-r} \approx 1$ cm^2 g^{-1}.

• The subsequent "red" (IR wavelength; $T_{\rm eff} \approx 2500$ K) luminosity of $L_{\rm read} \sim few \times 10^{40}$ erg s^{-1} of duration $t_{\rm peak} \sim 1$ week explained by $M_{\rm red} \approx 0.05 M_\odot$, $v_{\rm red} \approx 0.1$ c, $\kappa_{\rm heavy-r} \approx 10 - 100$ cm^2 g^{-1}.

Physically, what produced these ejecta? Comparing to Table 1:
• The red kilonova properties are consistent with an origin from a disk wind.

• The colors and high velocity of the blue kilonova are consistent with polar dynamical ejecta.
However, the high inferred mass is in tension with GR numerical simulations. This component might require something more exotic like a magnetized wind from the hypermassive neutron star (before it collapsed into a black hole).

Thermalization

We briefly comment on the thermalization efficiency $\epsilon_{\rm th}$ with which radioactive decay products share their energy with the bulk of the ejecta.

• The radioactive decay energy (Fig. 3) comes out in a variety of particles: $\beta-$decay electrons, neutrinos, gamma-rays, $\alpha-$particles, and fission fragments. Typical energies are in the MeV range.

• Neutrinos escape the ejecta immediately because of their very low cross section for interacting with matter.

• Gamma-rays interact with the ejecta mainly through inelastic electron scattering, with an opacity similar to Thomson scattering ($\kappa_\gamma \sim 0.1$ cm^2 g^{-1}); from equation (6), we see that gamma-rays will are trapped for roughly 1 day.

• Energetic charged particles ($\beta-$decay electrons, $\alpha-$particles, fission fragments) interact with the ejecta via Coulomb scattering off electrons or charged nuclei.

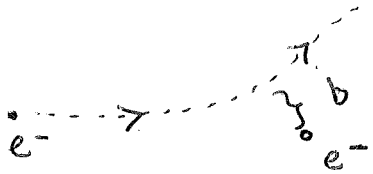

Example: $\beta-$decay electrons. The minimum impact parameter $b = b_{\rm min}$ for an electron of energy E to interact with a background electron of the same mass is

$$\frac{e^2}{b_{\rm min}} \approx E$$

To order-of-magnitude, the cross section for Coulomb interaction is

$$\sigma \sim \pi b_{\rm min}^2 \cdot \ln\Lambda \approx \pi \frac{e^4}{E^2} \ln\Lambda,$$

where $\ln\Lambda \sim 10$ is the Coulomb logarithm which accounts for the much more frequent weak collisions with impact parameters $\gg b_{\rm min}$.

The energy loss timescale of mildly relativistic β-decay electron of energy $E \approx m_e c^2$ and velocity $\lesssim c$ is therefore

$$t_{\rm e-e} \sim \frac{1}{n_e \sigma c} \sim \frac{E^2}{\pi c e^4 \ln\Lambda} \frac{A}{Z} \frac{m_p}{\rho_{\rm ej}} \underset{E \approx m_e c^2}{\approx} \frac{m_e^2 c^3 m_p}{e^4 \ln\Lambda} \frac{1}{\rho_{\rm ej}}$$
$$\approx 0.003 \quad {\rm days} \left(\frac{M_{\rm ej}}{0.01 M_\odot}\right)^{-1} \left(\frac{v_{\rm ej}}{0.1\,c}\right)^3 \left(\frac{t}{1\,{\rm day}}\right)^3 \qquad (13)$$

where $n_e = \rho_{\rm ej}/\mu_e$ is the electron density, $\mu_e = A m_p/Z$ is the mean mass per electron, and we have taken $\ln\Lambda = 10$.

On timescales $t_{\rm peak} \approx$ day-week, $t_{\rm e-e} \ll t_{\rm peak}$ and the beta-decay electrons will thermalize completely. This is no longer true once $t_{\rm e-e} \gtrsim t$, as occurs after a time

$$t_{\rm therm} \approx 19\ {\rm d} \left(\frac{M_{\rm ej}}{0.01 M_\odot}\right)^{1/2} \left(\frac{v_{\rm ej}}{0.1\,c}\right)^{-3/2}$$

Table 1: Sources of r-Process Ejecta in Binary Neutron Star Mergers

Ejecta Type	$M_{\rm ej}(M_\odot)$	$v_{\rm ej}(c)$	Y_e	KN Color	$M_{\rm ej}$ decreases with	Refs
Tidal Tails	$\sim 10^{-4}-10^{-2}$	$0.15-0.35$	$\lesssim 0.1$	Red (NIR)	$q=M_2/M_1$	e.g., 1,2
Polar Shocked	$\sim 10^{-4}-10^{-2}$	$0.15-0.35$	$\gtrsim 0.25-0.4$	Blue (visual)	$M_{\rm rem}/M_{\rm max}, R_{\rm ns}$	e.g., 3–5
Magnetar Wind	$\sim 10^{-3}-0.1M_\odot$	$\sim 0.1-1$ c	$\gtrsim 0.25$	Blue	$M_{\rm rem}/M_{\rm max}, B_{\rm rem}^{-1}$	6
Disk Outflows	$10^{-4}-0.07$	$0.03-0.1$	$\sim 0.1-0.4$	Blue+Red	$M_{\rm rem}/M_{\rm max}$	e.g., 7–10

(1) Rosswog et al. 1999; (2) Hotokezaka et al. 2013; (3) Bauswein et al. 2013; (4) Sekiguchi et al. 2016; (5) Radice et al. 2016; (6) Metzger et al. 2018; (7) Fernández & Metzger 2013; (8) Perego et al. 2014; (9) Just et al. 2015; (10) Siegel & Metzger 2017. Here $M_1, M_2, M_{\rm rem}$ are individual NS masses, and the total remnant mass, respectively. $B_{\rm rem}$ is the ordered large-scale magnetic field of the remnant HMNS.

Detailed Light Curve Model

In greater detail, one can solve for the time evolution of the ejecta internal energy $E_{\rm th}(t)$ and the resulting light curve $L_{\rm rad}(t)$ bolometric light curve by solving an ordinary differential equation (e.g. Metzger 2017),

$$\frac{dE_{\rm th}}{dt} = -\frac{E_{\rm th}}{R_{\rm ej}}\frac{dR_{\rm ej}}{dt} - L_{\rm rad} + \dot{Q}. \quad (14)$$

Here the first term accounts for PdV losses due to work done on the ejecta (adabiatic expansion). The second term,

$$L_{\rm rad} = \frac{E_{\rm th}}{t_{\rm diff}(t) + t_{\rm lc}}, \quad (15)$$

accounts for energy loss due to radiation, where $t_{\rm diff}$ is the diffusion time (eq. 4) and $t_{\rm lc} = R_{\rm ej}/c = (v_{\rm ej}/c)t$ limits the energy loss time to the light crossing time.

Note the following:

• The model can be generalized to include other forms of radioactivity (e.g. decay of free neutrons in the outer layers) or energy input from a central engine like an accreting black hole or the electromagnetic spin-down of a strongly magnetized neutron star.

Example: an accreting black hole could contribute a heating rate

$$\dot{Q}(t) = \epsilon_{\rm bh}\dot{M}_{\rm fb}c^2, \quad (16)$$

where $\dot{M}_{\rm fb} \propto t^{-5/3}$ is the rate of mass fall-back to the hole and $\epsilon_{\rm bh}$ is some efficiency factor.

• Thus far we have assumed the ejecta expands with a constant velocity $v_{\rm ej}$.
In detail, one should account for the acceleration of the ejecta. This is especially true if the amount of deposited energy $\dot{Q}dt$ at times $t \ll t_{\rm peak}$ exceeds the kinetic energy of the ejecta, $M_{\rm ej}v_{\rm ej}^2/2$. This correction is not important for radioactivity, but can be relevant for energy input from a long-lived magnetar.

References

Bauswein A., Goriely S., Janka H.-T., 2013, ApJ, 773, 78

Cowperthwaite P., et al., 2017, ApJL

Fernández R., Metzger B. D., 2013, MNRAS, 435, 502

Fernández R., Metzger B. D., 2016, Annual Review of Nuclear and Particle Science, 66, 23

Hotokezaka K., Kiuchi K., Kyutoku K., Okawa H., Sekiguchi Y.-I., Shibata M., Taniguchi K., 2013, Phys. Rev. D, 87, 024001

Just O., Bauswein A., Pulpillo R. A., Goriely S., Janka H.-T., 2015, MNRAS, 448, 541

Kasen D., Badnell N. R., Barnes J., 2013, ApJ, submitted, arXiv:1303.5788

Metzger B. D., 2017, Living Reviews in Relativity, 20, 3

Metzger B. D., Martínez-Pinedo G., Darbha S., Quataert E., Arcones A., Kasen D., Thomas R., Nugent P., Panov I. V., Zinner N. T., 2010, MNRAS, 406, 2650

Metzger B. D., Thompson T. A., Quataert E., 2018, ApJ, 856, 101

Perego A., Rosswog S., Cabezón R. M., Korobkin O., Käppeli R., Arcones A., Liebendörfer M., 2014, MNRAS, 443, 3134

Radice D., Galeazzi F., Lippuner J., Roberts L. F., Ott C. D., Rezzolla L., 2016, MNRAS, 460, 3255

Rosswog S., Liebendörfer M., Thielemann F., Davies M. B., Benz W., Piran T., 1999, A&A, 341, 499

Sekiguchi Y., Kiuchi K., Kyutoku K., Shibata M., Taniguchi K., 2016, Phys. Rev. D. , 93, 124046

Siegel D. M., Metzger B. D., 2017, ArXiv e-prints